Analytic Expression For the Electric Potential in the Plasma Sheath

TERRENCE E. SHERIDAN, JR. AND JOHN A GOREE

Abstract—**An expression for the spatial dependence of the electric potential in a collisionless and source-free planar plasma sheath is presented. This expression is derived in analogy with Child's law and approaches Child's law asymptotically as the potential drop ϕ_w across the sheath becomes large, $|e\phi_w/kT_e| > 10^4$. Here k is Boltzmann's constant, T_e is the electron temperature, and e is the electronic charge. Comparison with numerical solutions of the model equations indicate that the sheath thickness and potential variation predicted by this improved Child's law are accurate for $|e\phi_w/kT_e| > 10$. In contrast, we find that Child's law is accurate only when $|e\phi_w/kT_e| > 10^4$.**

I. Introduction

The plasma sheath is the localized electric field that separates a plasma from a material boundary. The plasma sheath serves to confine the more mobile species in the plasma and to accelerate the less mobile species out of the plasma. For the typical case where the electrons are more mobile than the positively charged ions, the electric field in the sheath points toward the boundary. The sheath thickness is parameterized by the Debye length λ_D.

In order for the potential in the sheath to decrease monotonically as we move from the plasma towards the boundary, ions must enter the sheath with a velocity at least as large as the ion acoustic velocity c_s [1]. As a consequence of this Bohm sheath criterion, a presheath is formed in the plasma with a potential drop on the order of $|kT_e/e|$, which accelerates the ions into the sheath. Here k is Boltzmann's constant, T_e is the electron temperature, and e is the electronic charge. The scale length of the presheath is set by either the mean free path for ions, or the scale length of the plasma, whichever is shorter [2].

When the potential drop across the sheath ϕ is large compared to $|kT_e/e|$, we can reasonably ignore the small potential drop across the presheath. The potential variation in the sheath is then approximated by Child's law [3]. However, severe approximations must be made to obtain Child's law, and the agreement between exact numerical solutions of Poisson's equation is within 1 percent only when $|e\phi/kT_e| > 10^4$.

In this paper we present an analytic expression for the potential variation in the plasma sheath. It is only slightly more complicated than Child's law, but is in much better agreement with exact numerical solutions. The model we use is appropriate for cathodic sheaths which are planar, collisionless, source-free, and in steady-state. We further assume that the boundary is perfectly absorbing and that the motion of electrons and ions to the boundary is not impeded by magnetic fields.

In the next section we outline the model of the plasma sheath under consideration, and in Section III we discuss approximate solutions to this model. The improved expression we derive provides useful information about the applicability of Child's law and the scaling of the sheath thickness with the potential drop across the sheath.

II. Sheath Model

We consider a widely used time-independent model for the potential in a planar plasma sheath ϕ as a function of position x [4]. One end of the plasma is terminated by a perfectly absorbing wall held at a negative potential ϕ_w. (Here, and throughout this paper, the subscript w will refer to the wall.) We choose the position of the wall to be $x = 0$ (see Fig. 1). Far from the wall there is a field-free and neutral plasma where $\phi = 0$. The density of electrons n_e and ions n_i are both equal to n_0 in the plasma. At some point $x = D$, where D is the sheath thickness, there is a transition from the nonneutral sheath to the neutral plasma. We assume that the sheath region is collisionless and source free. Ions enter the sheath as a monoenergetic beam with a velocity u_0. In this model u_0 must be greater than the ion acoustic velocity c_s in order that ϕ increases monotonically as we move away from the wall.

Since the sheath is source free, the ion density obeys an equation of continuity, $n_i v = n_0 u_0$, where v is the velocity of the ion beam in the sheath region. Further, since the sheath is collisionless, energy is conserved $Mv^2/2 = Mu_0^2/2 + e\phi$. Here M is the ion mass. Combining these two relations, we find that the ion density in the sheath is given by

$$n_i = n_0\left(1 - \frac{2e\phi}{Mu_0^2}\right)^{-1/2} \tag{1}$$

The electrons are assumed to be in thermal equilibrium; therefore, the electron density will follow the Boltzmann relation,

$$n_e = n_0 \exp\left(\frac{e\phi}{kT_e}\right). \tag{2}$$

Manuscript received May 18, 1989; revised July 24, 1989. This work was supported by the Iowa Department of Economic Development.

The authors are with the Department of Physics and Astronomy, The University of Iowa, Iowa City, IA 52242.

IEEE Log Number 8931372.

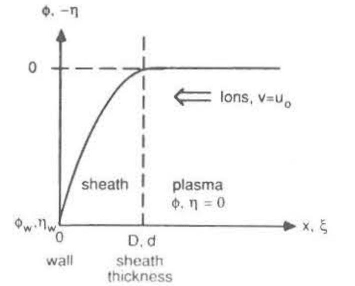

Fig. 1. Model system for the plasma sheath. The potential ϕ in the plasma sheath is plotted qualitatively as a function of the distance from the wall. Ions enter the sheath as a mono-energetic beam with a velocity u_0. Dimensionless quantities are shown to the right of their dimensional counterparts. Note that the sign of the dimensionless potential, $\eta = -e\phi/kT_e$, is opposite that of ϕ.

The potential must satisfy Poisson's equation,

$$\frac{d^2\phi}{dx^2} = -\frac{e}{\epsilon_0}(n_i - n_e)$$
$$= -\frac{en_0}{\epsilon_0}\left[\left(1 - \frac{2e\phi}{Mu_0^2}\right)^{-1/2} - \exp\left(\frac{e\phi}{kT_e}\right)\right] \quad (3)$$

where ϵ_0 is the permittivity constant. This nonlinear second-order ordinary differential equation is autonomous; i.e., $d^2\phi/dx^2$ does not depend explicitly on x. To completely specify the problem we need a value of u_0 and boundary conditions for ϕ. Appropriate boundary conditions are $\phi(0) = \phi_w$, and $\phi(x \to \infty) = 0$, as shown in Fig. 1.

Poisson's equation can be nondimensionalized by the following transformations:

$$\eta = -\frac{e\phi}{kT_e} \quad (4a)$$

$$\xi = \frac{x}{\lambda_D} = x\left(\frac{n_0 e^2}{\epsilon_0 kT_e}\right)^{1/2} \quad (4b)$$

$$\mathfrak{M} = \frac{u_0}{c_s} = \frac{u_0}{(kT_e/M)^{1/2}}. \quad (4c)$$

Here η is the dimensionless potential (note that the sign of η is opposite that of ϕ), ξ is the distance normalized by the Debye length, and $\mathfrak{M}$ is the Mach number. The dimensionless Poisson's equation for the potential variation in the sheath is

$$\eta'' = \left(1 + \frac{2\eta}{\mathfrak{M}^2}\right)^{-1/2} - e^{-\eta} \quad (5)$$

where η'' is the second derivative of η with respect to ξ. The first term on the right-hand side (RHS) is the dimensionless ion density, and the second term is the dimensionless electron density. The boundary conditions are $\eta(0) = \eta_w$, and $\eta(\xi \to \infty) = 0$. The Mach number must be specified. For this model the Bohm criterion requires that $\mathfrak{M} > 1$.

After multiplying by η', (5) can be integrated once to give

$$\eta' = -2^{1/2}\left[\mathfrak{M}^2\left(1 + \frac{2\eta}{\mathfrak{M}^2}\right)^{1/2} - \mathfrak{M}^2 + e^{-\eta} - 1\right]^{1/2} \quad (6)$$

where η', the dimensionless electric field, is negative, since η is positive at the wall and falls to zero in the plasma. We have incorporated the conditions that $\eta(\xi \to \infty) = 0$ and $\eta'(\xi \to \infty) = 0$. Because we must be given η_w and $\mathfrak{M}$ in order to completely specify a solution, both η' and η'', which are given by (6) and (5), can be evaluated at the wall. In fact, all derivatives of η can be evaluated at the wall. However, derivatives higher than first order all go to zero at the wall as η_w becomes large.

When might we expect this model to be a good description of the sheath? First, we have assumed that the sheath is collisionless. This is a good assumption when the mean free path for ion collisions is much larger than the sheath thickness. Secondly, we have ignored the presheath. We know from solutions to the plasma equation [2] that the maximum potential drop across the presheath is $\eta = 0.8539$. This suggests that the presheath can be treated in a simplified manner for $\eta \gg 1$. The potential in the plasma region is constant (there is no pre-sheath) when there is no source near the sheath [5], and no error is incurred by neglecting the presheath. Thirdly, it was assumed that the ion distribution entering the sheath is monoenergetic. The distribution of ion energies for ions born with zero energy is known to be very sharply peaked as the ions enter the sheath [6]. Fourthly, we have assumed that the electron density obeys the Boltzmann relation. Self [7] has argued that this assumption has a negligible effect on the results. Fifthly, we have assumed that there is no impediment (e.g., a magnetic field parallel to the wall) to the free flow of electrons and ions to the wall. Finally, we have assumed that the wall potential is time independent. The model will still hold for time-varying wall potentials provided that the oscillation frequency of the wall potential is less than the ion-plasma frequency [8].

The remainder of this paper considers approximate solutions to the sheath model presented above.

III. Approximate Analytic Solution

We consider the solutions to Poisson's equation (5) in the limits of small potential, $\eta \ll 1$, and large potential $\eta \gg 1$. When $\eta \ll 1$, the dependence of η on ξ is exponential. When $\eta \gg 1$ we find a power-law dependence for $\eta(\xi)$[1].

When $\eta \ll 1$ the leading terms in Poisson's equation give

$$\eta'' \approx \eta\left(1 - \frac{1}{\mathfrak{M}^2}\right). \quad (7)$$

[1]In the limit of $\mathfrak{M}^2 \gg \eta \gg 1$, Poisson's equation reduces to $\eta'' \approx 1$. This is the ion-matrix model, which has a quadratic solution. For this model the sheath width scales as $\eta_w^{1/2}$.

The asymptotic dependence of the potential on position for $\eta << 1$ is

$$\eta \sim \exp\left(-\xi \sqrt{1 - 1/\mathfrak{M}^2}\right). \tag{8}$$

In the opposite limit $\eta >> 1$, Poisson's equation reduces to

$$\eta'' \approx \mathfrak{M}(2\eta)^{-1/2}. \tag{9}$$

Child [3] found that the solution to (9), subject to the boundary conditions at the wall $\eta(0) = \eta_w$ and at the plasma-sheath interface $\eta(d) = 0$, is

$$\eta(\xi) = \left(\frac{9}{4}\frac{\mathfrak{M}}{\sqrt{2}}\right)^{2/3} (d - \xi)^{4/3}, \qquad \xi \le d$$
$$= 0, \qquad \xi > d. \tag{10}$$

The sheath thickness d is given by

$$d = \frac{4}{3}\frac{\eta_w^{3/4}}{2^{3/4}\mathfrak{M}^{1/2}} \tag{11}$$

and is the thickness of the region where the electron density is negligible. Equations (10) and (11) taken together are called *Child's law*.

Child's law relates three quantities: The wall potential η_w, the sheath thickness d, and the Mach number $\mathfrak{M}$. The Mach number is related to the current density for ions entering the sheath. Hence, Child's law is often used to determine the current density flowing into a sheath, $J_i \propto en_0u_0 = en_0c_s\mathfrak{M}$, for given values of η_w and d [9], where d must be determined without using (11). We, however, are interested in the spatial variation of the potential in the plasma sheath.

Fig. 2 compares the spatial variation in the potential predicted by Child's law with an exact numerical solution of Poisson's equation for $\eta_w \le 800$ and $\mathfrak{M} = 1.05$. The exact solution is found by integrating η', given by (6), from the wall towards the plasma using a Runge–Kutta method [10]. The exact solution's power-law nature for $\eta >> 1$ and exponential nature for $\eta << 1$ are clearly visible. The exponential solution is dominant for $\eta < 0.1$. The agreement between Child's law and the exact solution is increasingly poor as the transition from the sheath to the plasma is approached.

We want a more accurate analytic expression for $\eta(\xi)$ than Child's law. Instead of looking for an exact solution to an approximate equation, we look for an approximate solution to the exact equation. The power-law form of Child's law suggests that we try

$$\eta(\xi) = a(d - \xi)^b, \qquad \xi \le d$$
$$= 0, \qquad \xi > d. \tag{12}$$

Note that $\eta'(d) = 0$. To find values for the coefficients a, b, and d, we require that $\eta(0) = \eta_w$, $\eta'(0) = \eta'_w$, and $\eta''(0) = \eta''_w$. Solving the resulting equations, we find that b, d, and a are given by

$$b = \frac{1}{1 - \eta_w\eta''_w/\eta'^2_w} \tag{13a}$$

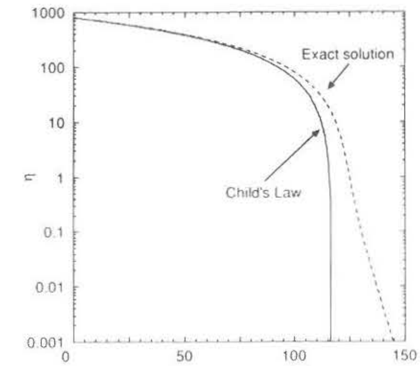

Fig. 2. Semi-log plot for the dimensionless potential η in the sheath as a function of the dimensionless distance from the wall ξ for an exact numerical solution and Child's law with $\mathfrak{M} = 1.05$. Note that η is a positive quantity, in contrast to the actual potential ϕ which is negative, as exhibited in Fig. 1. Agreement between Child's law and the exact solution is good in the power law regime $\eta >> 1$. Agreement is poor in the exponential regime $\eta << 1$.

$$d = -b\frac{\eta_w}{\eta'_w} = \frac{\eta'_w\eta_w}{\eta_w\eta''_w - \eta'^2_w} \tag{13b}$$

$$a = \frac{\eta_w}{d^b}. \tag{13c}$$

Equations (12) and (13a)–(13c) together with (5) and (6) for the derivatives make up what we will call the *improved* Child's law, because of its superior agreement with the exact numerical solutions for $\eta_w < 10^4$.

When the asymptotic values for η'_w and η''_w,

$$\eta'_{wa} \approx -2^{3/4}\mathfrak{M}^{1/2}\eta_w^{1/4} \tag{14}$$

$$\eta''_{wa} \approx \mathfrak{M}(2\eta_w)^{-1/2} \tag{15}$$

are substituted into (12) and (13), Child's law is recovered. Hence, in the asymptotic limit the improved Child's law approaches Child's law.

Fig. 3 shows the difference between the exponent b (equation (11a)) and the asymptotic value of $4/3$, which is used in Child's law. We see that the difference is significant even at $\eta_w = 100$, and that b goes to its asymptotic value as $\eta_w^{-1/2}$. This indicates that Child's law is only accurate for $\eta_w^{1/2} >> 1$.

The sheath thickness for Child's law, the improved law, and the exact solution are shown plotted against η_w in Fig. 4. As the wall potential becomes large the improved law exhibits the same $3/4$ power scaling of d with η_w that Child's law shows. There is a minimum in the sheath thickness at $\eta_w \approx 6$ for the improved law. (The exact position depends on $\mathfrak{M}$.) This occurs as the character of the exact solution changes from power law to exponential, and is due to the attempt of the improved law to better fit the exponential by increasing b (see Fig. 3). However, if we ignore this unphysical increase in d for small values of η_w, the improved Child's law fits the exact numerical solution well even for η_w on the order of 10.

Fig. 5(a)–(c) compares the spatial variations in the electric potential found by using Child's law, the improved Child's law, and the exact solution for values of $\eta_w = 10$, 30, and 100 and $\mathfrak{M} = 1.05$. We see that even

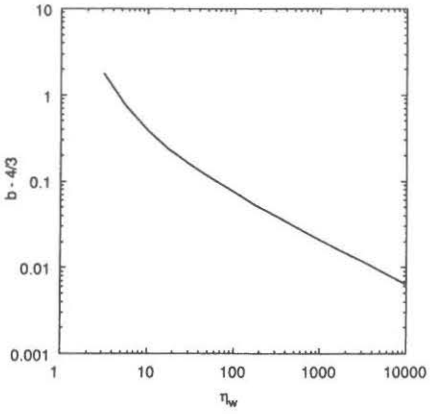

Fig. 3. Difference between the exponent in the improved Child's law b and the asymptotic value of $4/3$ used in Child's law plotted against the wall potential η_w, with $\mathfrak{M} = 1.05$. Note that this difference goes to zero only as $\eta_w^{-1/2}$.

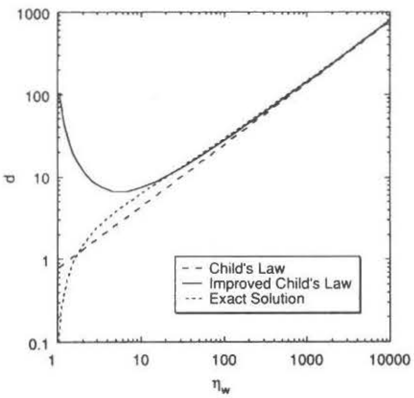

Fig. 4. Dimensionless sheath thickness d for Child's law, the improved Child's law, and the exact numerical solution plotted against the wall potential η_w, with $\mathfrak{M} = 1.05$. For the exact solution the sheath thickness is chosen to be the distance from the wall to the point where $\eta = 1$.

at $\eta_w = 100$ (Fig. 5(c)), the improved expression is still noticeably different from Child's law and in much better agreement with the exact solution. Because of the exponential nature of the exact solution for $\eta < 1$, power-law solutions, such as Child's law and the improved Child's law, fail for small η. However, by allowing the exponent b to vary with η_w, the improved law gives much better agreement with the exact solution than does Child's law. This improved agreement is most apparent for smaller values of the wall potential (i.e., $\eta_w = 10$ in Fig. 5(a)).

Finally, by expanding both the exponent b and the sheath thickness d for $\eta_w >> 1$, we can determine how large η_w must be for the Child's law and the improved law to be in good agreement. We find that

$$b \approx \frac{4}{3}\left[1 + \frac{1}{3(2\eta_w)^{1/2}}\left(\mathfrak{M} + \frac{1}{\mathfrak{M}}\right)\right] \tag{16}$$

$$d \approx \frac{4}{3}\frac{\eta_w^{3/4}}{2^{3/4}\mathfrak{M}^{1/2}}\left[1 + \frac{5}{2^{3/2}3}\frac{1}{\eta_w^{1/2}}\left(\mathfrak{M} + \frac{1}{\mathfrak{M}}\right)\right]. \tag{17}$$

The values of b and d predicted by (16) and (17) asymptotically approach those of Child's solution for $\eta_w >> 1$,

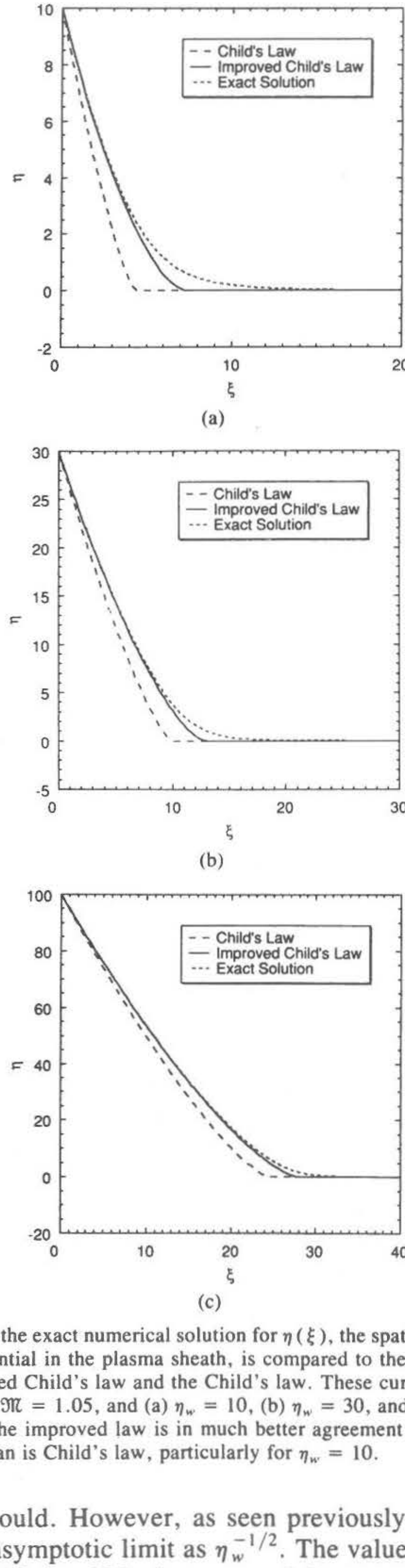

Fig. 5. Here the exact numerical solution for $\eta(\xi)$, the spatial dependence of the potential in the plasma sheath, is compared to the predictions of the improved Child's law and the Child's law. These curves were computed with $\mathfrak{M} = 1.05$, and (a) $\eta_w = 10$, (b) $\eta_w = 30$, and (c) $\eta_w = 100$. Note that the improved law is in much better agreement with the exact solution than is Child's law, particularly for $\eta_w = 10$.

as they should. However, as seen previously, they only go to the asymptotic limit as $\eta_w^{-1/2}$. The value of b found by using (16) is within 1 percent of the asymptotic value for $\eta_w = 2200$ (assuming that $\mathfrak{M} + 1/\mathfrak{M} = 2$). The sheath thickness predicted from Child's law is within 1 percent of (17) for $\eta_w = 12\,000$. We can also expand the electric field for $\eta >> 1$ to give

$$\eta' \approx -2^{3/4}\mathfrak{M}^{1/2}\eta^{1/4}\left[1 - \frac{1}{2^{3/2}\eta^{1/2}}\left(\mathfrak{M} + \frac{1}{\mathfrak{M}}\right)\right]. \tag{18}$$

At the wall this expression also shows the same $\eta_w^{-1/2}$ convergence as (16) and (17). For η_w' to be within 1 percent of its asymptotic value, we need $\eta_w = 5000$. We conclude that Child's law only provides a good approximation (within 1 percent) for the potential variation within the sheath when the potential drop across the sheath η_w is greater than 10^4.

IV. Summary

We have presented an improved Child's law (equations (12) and (13)), together with (5) and (6), for the time-independent spatial variation of the electric potential for the source-free, collisionless, cathodic plasma sheath. It provides a significant improvement over Child's law when $|e\phi/kT_e|$ at the wall is less than 10^4. The two expressions agree in the asymptotic limit, and the improved expression is no more difficult to evaluate once the coefficients a, b, and d (equations (13a)–(13c)) have been calculated.

Acknowledgment

The authors wish to acknowledge useful discussions with R. Merlino.

References

[1] D. Bohm, in *The Characteristics of Electrical Discharges in Magnetic Fields*, A. Guthrie and R. K. Wakerling, Eds. New York: McGraw-Hill, 1949, pp. 77–86.
[2] L. Tonks and I. Langmuir, "A general theory of the plasma of an arc," *Phys. Rev.*, vol. 34, pp. 876–922, Sept. 1929.
[3] C. D. Child, "Discharge from hot CaO," *Phys. Rev.*, vol. 32, pp. 492–511, 1911.
[4] F. F. Chen, *Introduction to Plasma Physics*. New York: Plenum, 1974, pp. 244–249.
[5] G. A. Emmert, R. M. Wieland, A. T. Mense, and J. N. Davidson, "Electric sheath and presheath in a collisionless, finite ion temperature plasma," *Phys. Fluids*, vol. 23, pp. 803–812, Apr. 1980.
[6] F. F. Chen, "Electrostatic stability of a collisionless plane discharge," *Il Nuovo Cimento*, vol. 26, pp. 4530–4548, Nov. 1962.
[7] S. A. Self, "Exact solution of the collisionless plasma-sheath equation," *Phys. Fluids*, vol. 6, pp. 1762–1768, Dec. 1963.
[8] M. H. Cho, N. Hershkowitz, and T. Intrator, "Temporal evolution of collisionless sheaths," *J. Vac. Sci. Technol.*, vol. A6, pp. 2978–2986, Sept./Oct. 1988.
[9] P. Martin and G. Donoso, "A new Langmuir-Child equation including temperature effects," *Phys. Fluids*, vol. B1, pp. 247–251, Jan. 1989.
[10] C. E. Roberts, Jr., *Ordinary Differential Equations: A Computational Approach*. Englewood Cliffs, NJ: Prentice-Hall, 1979, pp. 111–116.

*